Chapter 5: Modeling and validation of a recovery model via coupling between myelinated and demyelinated nerve fibers using toad nerve model

Contents

It always seems impossible until it's done.
-Nelson Mandela

5.1 Introduction

The demyelination of peripheral nervous system (PNS) results in nerve disorder such as slow and inefficient propagation of nerve signals having sequences of action potential as seen in chronic inflammatory demyelinating polyneuropathy (CIDP) [1, 2], Guillain-Barre syndrome (GBS) patients [3, 4]. Demyelination mainly provides defective structure or dysfunction of the myelin sheath. Treatment of these neuro diseases requires strategies to repair the damaged myelin sheath of the nerves.

Rapid recovery of dysfunction of the myelin sheath has become an important problem in neuroscience for efficient treatment of these diseases [5, 6]. Previous studies show that spectrin (αII and βII) inhibit peripheral nerve remyelination and the regulation of spectrin remyelination is very much complex providing slow recovery of myelin sheath. Moreover it is difficult to control activities of cytoskeleton of Schwann cell acting as myelinating glia [7-9]. Cell replacement therapy and transplantation of stem cells provides an effective treatment due to its self renewing and multipotential nature of cells and is used to replace the lost or damaged nerve cells [10, 11].

Keeping the above issues in view, this chapter deals with designing of a coupled electric circuit model between a single demyelinated nerve with a myelinated nerve. The recovery in nerve conduction velocity (NCV) due to demyelination is shown theoretically via simulation. The work is also extended to the experimental validation on a frog model where its sciatic nerve was isolated and demyelinated using crude venom of *Naja kaouthia* (Nk). The venom treated demyelinated nerve is coupled with a normal myelinated sciatic nerve of toad to form a coupled model and the properties of nerve conduction signals were examined using AD instrument.

5.2 Nerve fiber coupling

Two parallel and closely situated nerves can interact with each other ephaptically and thus either of the nerves can create an impact on the electrodynamics of other nerve and the vice-versa [12]. It is already reported that two parallel and closely placed nerves can interact with each other ephaptically, thus creating impact on electrodynamics of one another [13-15]. Since 19^{th} century, many theories and experiments were evolved or performed to show

transmission of electrical pulses (i.e. sequences of action potential) through nerve fiber influencing with activity of the surrounding nerve fiber [16-18]. Many experiments also demonstrated the firing of a primary nerve produces a secondary excitation upon the adjacent secondary nerve by ephaptic interaction [14-17] as shown in Fig-5.1(a) and (b).

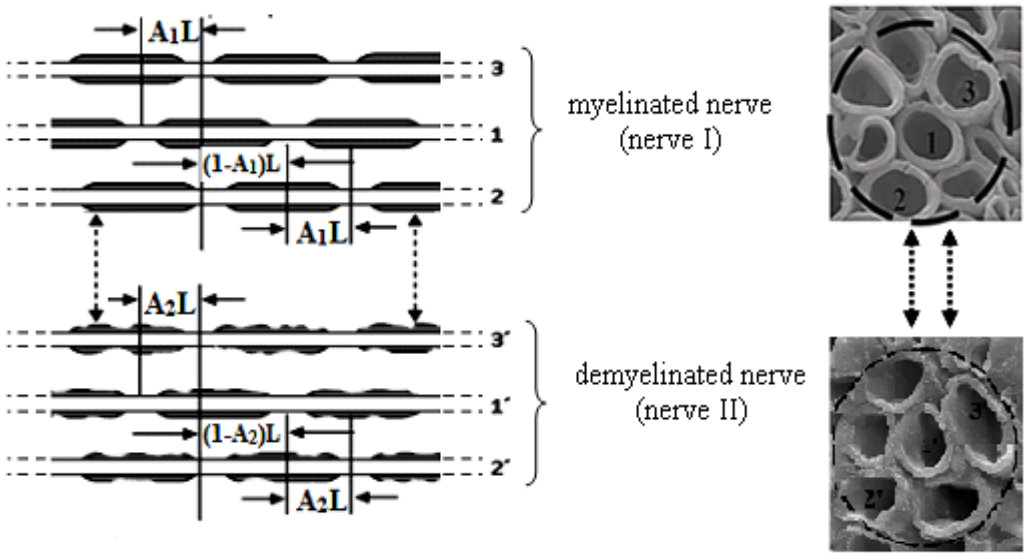

(a) (b)

Figure 5.1: (a) A myelinated nerve (nerve I) being coupled with a demyelinated nerve (nerve II) and (b) image of nerve I and nerve II to be coupled for the formation of coupled nerve model obtained from scanning electron microscope (SEM).

5.2.1 Electric circuit model of coupling

The development of Hodgkin-Huxley (H-H) model of nerve has led a foundation for many scientists to report and demonstrate many electric circuit models of demyelinated nerves to study the physiological properties of the nerves [19-21]. In this section, we a coupling model of two nerves- nerve I (normal), and nerve II (demyelinated) being ephaptically coupled with each other is represented by an electric circuit model as shown in Fig-5.1.

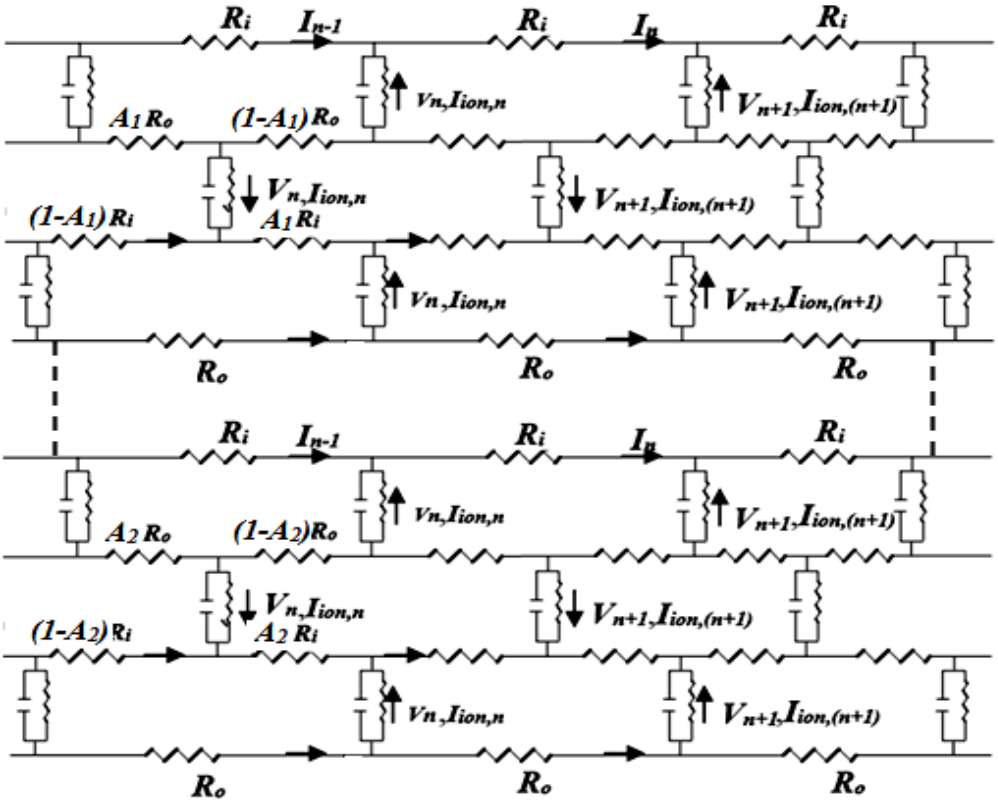

Figure 5.2: An electric circuit model of a couple nerve fibers.

The model reflects on alignment parameter A_1 coupling constant α_1 in normal nerve and alignment factor A_2 and ephaptic coupling constant α_2 in demyelinated nerve respectively (as shown in Fig-5.2). Fig-5.2 represents an electrical circuit model of coupling between nerve I and nerve II (both nerve I and nerve II considers electrical ephaptic interaction of axon I with other surrounded axons). The I_n and V_n are nodal ionic current and voltage at node n whereas I_{n+1} and V_{n+1} are nodal ionic current and voltage at node $(n+1)$ respectively. In the circuit the voltage V_n at node n depends on V_{Na}, V_{Kf}, V_{Ks} and V_L which are Nernst potentials of sodium, fast potassium, slow potassium and leakage ion at which corresponding currents return to zero. The equivalent resistance in the model due to the effect of the myelinated nerve and demyelinated nerve with demyelination factor γ_1 and γ_2 respectively is

$$R = [(R_i + R_o)(1+\gamma_1)] + [(R_i + R_o)(1+\gamma_2)]$$

$$R = (R_i + R_o)(2+\gamma_1+\gamma_2) \qquad (5.1)$$

The total demyelination factor (γ) in the coupled model is given by $\gamma=\gamma_1+\gamma_2$. But $\gamma_1=0$, for myelinated nerve in the model. Therefore, $\gamma=\gamma_2$. Thus the total resistance in equation (5.1) becomes

$$R = (R_i + R_o)(2+\gamma) \tag{5.2}$$

And the increase in capacitance due to total demyelination in the model is $C(2+\gamma)$, while the ionic conductances are increased by $G_{Na}(2+\gamma)$, $G_{Kf}(2+\gamma)$, $G_{Ks}(2+\gamma)$, and $G_L(2+\gamma)$ respectively due to Na^+, fast K^+, slow K^+ and ions responsible for leakage currents. The currents incorporation with the total demyelinating factor γ in terms of conductance and potential with cubic polynomial function approximation and considering resting potential zero at equilibrium can be denoted as-

$$I_{Na} = \left(\frac{G_{Na}(2+\gamma)}{V_{Na}(V_{Na} - V_{th}^{Na})}\right)V_n(V_n - V_{th}^{Na})(V_n - V_{Na})$$

$$I_{Kf} = \left(\frac{G_{Kf}(2+\gamma)}{V_K(V_K - V_{th}^{Kf})}\right)V_n(V_n - V_{th}^{Kf})(V_n - V_K)$$

$$I_{Ks} = \left(\frac{G_{Ks}(2+\gamma)}{V_K(V_K - V_{th}^{Ks})}\right)V_n(V_n - V_{th}^{Ks})(V_n - V_K)$$

$$I_L = \left(\frac{G_L(2+\gamma)}{V_L(V_{Na} - V_{th}^{L})}\right)V_n(V_n - V_{th}^{L})(V_n - V_L) \tag{5.3}$$

Where, I_{Na}, I_{Kf}, I_{Ks} and I_L are the corresponding ionic currents due to flow of sodium ions, fast potassium and slow potassium and leakage ions such as chlorine and calcium ions respectively.

5.2.2 Estimation of NCV in coupled model

As discussed in chapter-3 and chapter-4, the current at node n-1 and node n is written as-

$$I_{n-1} = (V_{n-1} - V_n)/\{(R_i + R_o)(2-\gamma)\} \tag{5.4}$$

$$I_n = (V_n - V_{n+1})/\{(R_i + R_o)(2-\gamma)\} \tag{5.5}$$

Applying Kirchoff's law of current, the current equation at the nodes can be represented as

$$I_{n-1} - I_n = C(2+\gamma)\frac{\partial V_n}{\partial t} + I_{ion,n} \tag{5.6}$$

From equations (5.4), (5.5) and (5.6) and equating the values of total resistance, the standard equation becomes

$$\{1/R(2-\gamma)\}[V_{n-1} - 2V_n + V_{n+1}] = C(2+\gamma)\frac{\partial V_n}{\partial t} + I_{ion,n} \tag{5.7}$$

From equation (5.3), equation (5.7) can be represented in the standard notation as shown below

$$\begin{aligned}\{1/R(2-\gamma)\}[V_{n-1} - 2V_n + V_{n+1}] &= C(2+\gamma)\frac{\partial V_n}{\partial t} \\ &+\left(\frac{G_{Na}(2+\gamma)}{V_{Na}(V_{Na} - V_{th}^{Na})}\right)V_n(V_n - V_{th}^{Na})(V_n - V_{Na}) \\ &+\left(\frac{G_{Kf}(2+\gamma)}{V_K(V_K - V_{th}^{Kf})}\right)V_n(V_n - V_{th}^{Kf})(V_n - V_K) \\ &+\left(\frac{G_{Ks}(2+\gamma)}{V_K(V_K - V_{th}^{Ks})}\right)V_n(V_n - V_{th}^{Ks})(V_n - V_K) \\ &+\left(\frac{G_L(2+\gamma)}{V_L(V_{Na} - V_{th}^{L})}\right)V_n(V_n - V_{th}^{L})(V_n - V_L)\end{aligned} \tag{5.8}$$

The dynamic equation for (5.8) can represented by replacing $1/RC(2^2-\gamma^2)$ as a diffusion constant, D. Equation (5.8) becomes

$$D[V_{n-1}-2V_n+V_{n+1}]=\frac{\partial V_n}{\partial t}$$

$$+\{1/C(2+\gamma)\}[(\frac{G_{Na}(2+\gamma)}{V_{Na}(V_{Na}-V_{th}^{Na})})V_n(V_n-V_{th}^{Na})(V_n-V_{Na})$$

$$+(\frac{G_{Kf}(2+\gamma)}{V_K(V_K-V_{th}^{Kf})})V_n(V_n-V_{th}^{Kf})(V_n-V_K)$$

$$+(\frac{G_{Ks}(2+\gamma)}{V_K(V_K-V_{th}^{Ks})})V_n(V_n-V_{th}^{Ks})(V_n-V_K)$$

$$+(\frac{G_L(2+\gamma)}{V_L(V_{Na}-V_{th}^{L})})V_n(V_n-V_{th}^{L})(V_n-V_L)] \quad (5.9)$$

The equation (5.9) represents a discrete reaction diffusion equation of myelinated nerve. Equation (5.9) can be written in continuum limit as partial differential equation which is given below,

$$D\frac{\partial^2 t}{\partial x^2}-\frac{\partial V_n}{\partial t}=\{1/C(2+\gamma)\}[(\frac{G_{Na}(2+\gamma)}{V_{Na}(V_{Na}-V_{th}^{Na})})V_n(V_n-V_{th}^{Na})(V_n-V_{Na})$$

$$+(\frac{G_{Kf}(2+\gamma)}{V_K(V_K-V_{th}^{Kf})})V_n(V_n-V_{th}^{Kf})(V_n-V_K)$$

$$+(\frac{G_{Ks}(2+\gamma)}{V_K(V_K-V_{th}^{Ks})})V_n(V_n-V_{th}^{Ks})(V_n-V_K)$$

$$+(\frac{G_L(2+\gamma)}{V_L(V_{Na}-V_{th}^L)})V_n(V_n-V_{th}^L)(V_n-V_L)] \tag{5.10}$$

As described in chapter 3 and chapter 4, the coupling constant α in the coupled model is given by

$$\alpha=\frac{R_i(2-\gamma)}{R_i(2-\gamma)+R_O(2-\gamma)A(N-1)} \tag{5.11}$$

Where, $R=R_i(2-\gamma)+R_o(2-\gamma)A(N-1)$ and $A=A_1+A_2$, is the total alignment factor in the model. Thus using equation (5.11), the equivalent resistance for the model in terms of α can be written as

$$R=\frac{R_O(2-\gamma)A(N-1)}{(1-\alpha)} \tag{5.12}$$

Thus, the NCV in the demyelinated nerve using traveling wave solutions of equation with leading edge approximation (as discussed in previous chapters) in terms of coupling constant and alignment factor in a bundle of axons in the nerve fiber is given by-

$$v_C=\sqrt{\frac{G_{Na}(2+\gamma)(1-\alpha)}{R_O(2-\gamma)A(N-1)\{C(2+\gamma)\}^2}}\frac{V_{Na}-2V_{th}^{Na}}{\sqrt{2V_{Na}}}(2-\gamma)$$

$$+\sqrt{\frac{G_{Kf}(2+\gamma)(1-\alpha)}{R_O(2-\gamma)A(N-1)\{C(2+\gamma)\}^2}}\frac{V_K-2V_{th}^{Kf}}{\sqrt{2V_K}}(2-\gamma)$$

$$+\sqrt{\frac{G_{Ks}(2+\gamma)(1-\alpha)}{R_O(2-\gamma)A(N-1)\{C(2+\gamma)\}^2}}\frac{V_K-2V_{th}^{Ks}}{\sqrt{2V_K}}(2-\gamma)$$

$$+\sqrt{\frac{G_L(2+\gamma)(1-\alpha)}{R_O(2-\gamma)A(N-1)\{C(2+\gamma)\}^2}}\frac{V_L-2V_{th}^L}{\sqrt{2V_L}}(2-\gamma) \tag{5.13}$$

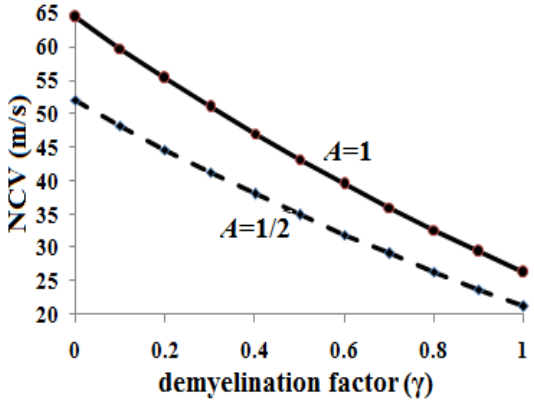

Figure 5.3: Estimation of NCV in the coupled nerve for aligned (A=1) and misaligned (A=1/2) axons in the model.

Fig-5.3 represents the comparison of NCV estimated for aligned and misaligned axons in the bundle of a coupled nerve using equation (5.13). It is clearly seen that the NCV for aligned axons have higher values than the NCV estimated for misaligned axons in the coupled model. As discussed in chapter 3 and chapter 4, the NCV for a nerve depends directly on the alignment factor of the nerve.

5.3 Formation of a coupled nerve model

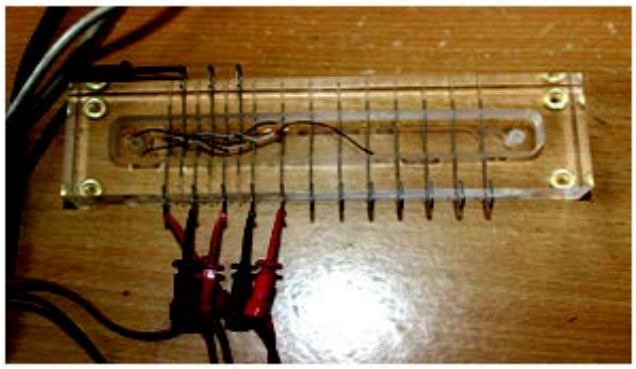

Figure 5.4: A coupled nerve in a nerve chamber.

The procedure for the isolation of sciatic nerves of toad and the process of demyelination with the use of Nk venom remains the same as discussed in previous works of chapter 3 and chapter 4. Therefore the materials including the reagents of analytical grade,

description about snake venom assay and the instrumental set up to record the electro neuro signals from the isolated nerves have been clearly described in previous chapters. For the formation of coupled nerve using toad model, 36 toads of same groups (~1-2months) are collected and divided into four groups namely A, B, C and D. The extracted toad sciatic nerves of A are considered as control (normal and myelinated) without the treatment of snake venom while the nerves of B, C and D are demyelinated with 0.1μg/ml, 1.0μg/ml and 10μg/ml crude Nk venom. SEM imaging of the isolated nerves is performed to confirm demyelination by morphological change in the myelin sheaths with reduced myelin thickness. The nerves were subjected to 2.5% gluteraldehyde for 4hr which is immediately followed by the secondary fixation of the same nerve using 1% OsO_4 (Osmium tetroxide) for 4hr for better penetration. The change in the myelin structure and its reduced myelin thickness is almost same as observed in section 4.4.1.8 of chapter 4. Thus, the data collected from SEM confirms the process of demyelination by treatment with different concentrations of Nk venom. The CAP recordings were calibrated separately for the nerves of all the groups using AD instrument and their NCV are estimated from the signals using latency-distance calibration method.

Each of the demyelinated nerves of B, C and D are interacted with the nerves of A by tying the proximal and distal ends of the nerves with surgical threads in order to form a coupled like structure as shown in Fig-5.3. Under the same experimental condition of 1Hz for duration of 0.1ms as applied in case of myelinated and demyelinated nerves, the electro neuro signals are extracted in the instrument to record CAP and thereby estimate the NCV in the coupled model. The experiments are performed 5-6 times and similar experiments were carried out separately with purified Nk-PLA_2 and 3FTx to study its neurotoxic effects in the coupled model.

5.4 Results

Table 5.1: Theoretical estimation of NCV (m/s) in demyelinated nerves and coupled nerves for different alignment factor with respect to human nerve parameters

Demyelination factor (γ)	NCV (m/s)			
	A=1/2		*A*=1	
	Demyelinated nerve	Coupled nerve	Demyelinated nerve	Coupled nerve
0	40.21	52.03	52.52	64.41
0.1	34.50	48.24	45.07	59.71
0.2	29.36	44.65	38.35	55.27
0.3	24.68	41.24	32.24	51.05
0.4	20.39	38.00	26.63	47.04
0.5	16.41	34.91	21.44	43.21
0.6	12.71	31.95	16.61	39.54
0.7	9.25	29.11	12.08	36.03
0.8	5.99	26.39	7.83	32.66
0.9	2.92	23.77	3.81	29.42
1	-	21.24	-	26.30

For the recovery of disorder of peripheral nerves due to demyelination experimentally, sciatic nerves isolated from toad are stored in Ringer's solution and keeping moist condition inside the nerve chamber, nerve conduction experiments are performed by using AD instruments. The reduction of myelin thickness of sciatic nerves with treatment of Nk venom of concentration 0.1µg/ml, 1µg/ml and 10µg/ml is already shown in the previous work (also from SEM images shown in Fig. 4.7(b)-(d) of chapter 4). Due to demyelination, NCV decreases below its normal values as obtained from nerve conduction signals of proximal and distal action potential of sciatic nerves treated with same concentration Nk crude venom (Fig-5.4(A)-(C)). The neuro signals recorded from demyelinated nerves treated with 0.1µg/ml, 1µg/ml and 10µg/ml of Nk venom, the NCV are found to be 26.62±0.58m/s, 18.25±0.25m/s and 15.87±0.15m/s for their corresponding venom concentrations as shown in Table-5.2.

Table 5.2: Estimation of NCV for various concentrations of Nk crude venom

Estimation of NCV (m/s)						
No. of observations	**Crude venom concentrations**					
	0.1µg/ml		**1µg/ml**		**10µg/ml**	
	Before coupling	**After coupling**	**Before coupling**	**After coupling**	**Before coupling**	**After coupling**
I	26.32	40.49	18.02	37.43	16.09	35.01
II	26.65	40.55	18.43	37.36	15.97	34.69
III	26.17	40.26	18.60	37.63	15.93	34.77
IV	25.99	40.29	18.13	37.60	15.76	34.74
V	27.49	40.30	18.11	37.44	15.72	34.91
VI	27.09	40.22	18.21	37.52	15.77	34.99
NCV with SD	26.62±0.58	40.36±0.12	18.25±0.22	37.50±0.11	15.87±0.15	34.85±0.14

When the same are coupled with myelinated nerves, an increase in the NCV by 40.36±0.12m/s, 37.50±0.11m/s and 34.85±0.14m/s are observed in the coupled model for the same amount of venom concentrations of the demyelinated nerve as shown in Fig-5.4(a)-(c) and Table-5.2. There is also the reduction of amplitude of both proximal and distal CAP due to treatment of Nk-crude venom as reported in previous works. Nk-PLA_2 of crude venom is mainly responsible for the reduction of myelin thickness (as shown in Table-5.3). The reduction of NCV affected by purified Nk-PLA_2 is found to be 25.62±0.81m/s, 17.10±0.13m/s and 14.46±0.58m/s for 0.1µg/ml, 1.0µg/ml and 10µg/ml of Nk-PLA_2 respectively. When the nerve is coupled with a normal nerve, the increase value of NCV is obtained to be 39.24±0.26m/s, 36.36±0.35m/s and 33.66±0.38m/s respectively. whereas weak three finger neurotoxin (3FTx) of crude venom affects in reduction of CAP amplitude due to blocking of Na^+ and K^+ channels as discussed here later.

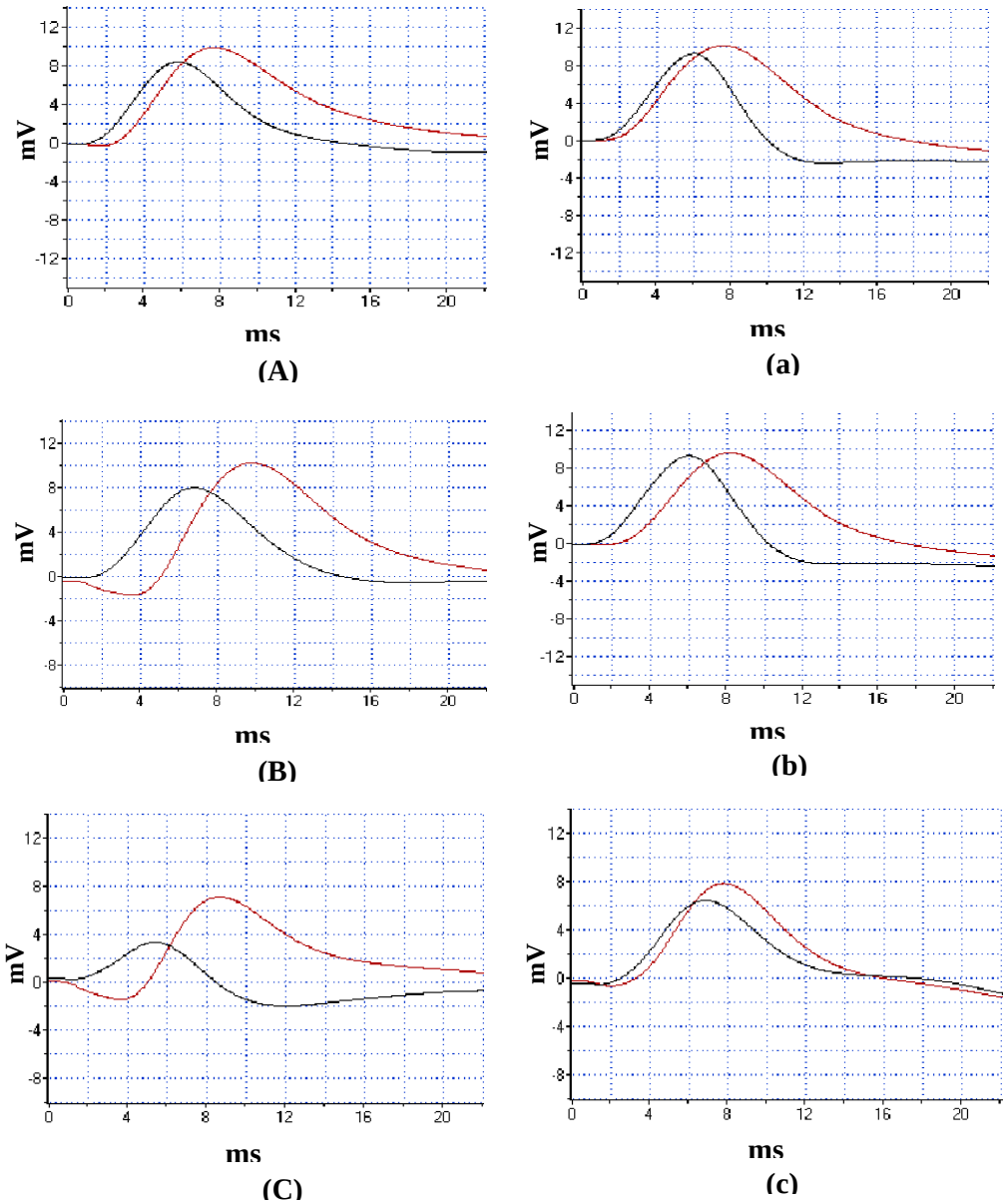

Figure 5.4: Electro neuro signals in demyelinated and coupled nerve.

Table 5.3: Estimation of NCV for various concentrations of purified Nk-PLA_2

Estimation of NCV (m/s)						
No. of observations	**Concentrations of purified Nk-PLA_2**					
	0.1µg/ml		**1µg/ml**		**10µg/ml**	
	Before coupling	**After coupling**	**Before coupling**	**After coupling**	**Before coupling**	**After coupling**
I	25.12	39.45	16.92	36.49	15.39	34.19
II	25.06	39.57	17.13	36.36	14.91	33.89
III	25.32	38.96	17.06	35.93	14.45	33.75
IV	25.99	39.19	16.99	35.99	13.98	33.14
V	26.19	39.36	17.21	36.84	14.02	33.31
VI	26.03	38.92	17.27	36.57	14.00	33.69
NCV with SD	25.62±0.81	39.24±0.26	17.10±0.13	36.36±0.35	14.46±0.58	33.66±0.38

5.4.1 Recovery of disorder

For the recovery from dysfunction of Nk crude venom treated nerve coupling of the same is made with normal sciatic nerve and performed nerve conduction experiment on the same coupled nerves. The NCV in coupled nerve (combination of nerve I treated with crude venom and normal nerve II) increases by ~34% for 0.1µg/ml, ~51% for 1µg/ml and ~54% for 10µg/ml respectively whereas a nerve treated with purified Nk-PLA_2 is used in the coupled nerve, the increase in NCV are found to be ~35% for 0.1µg/ml, ~53% for 1µg/ml and ~57% for 10µg/ml of purified Nk-PLA_2 respectively. The experimental values of NCV of demyelinated nerves and coupled nerves varies in a similar way as observed in the theoretical model obtained in Table-5.1 and shown in Fig-5.6(a) and (b) by using equation (5.11) with standard parameters described in Table-3.1 (chapter 3).

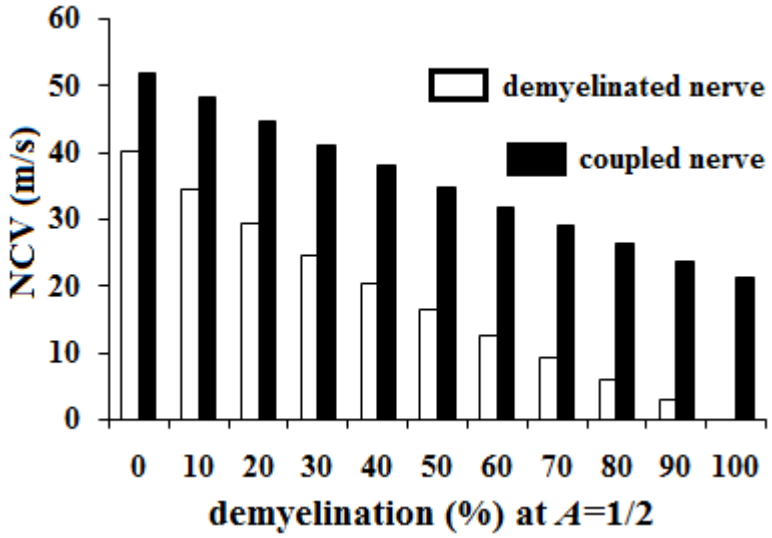

(a)

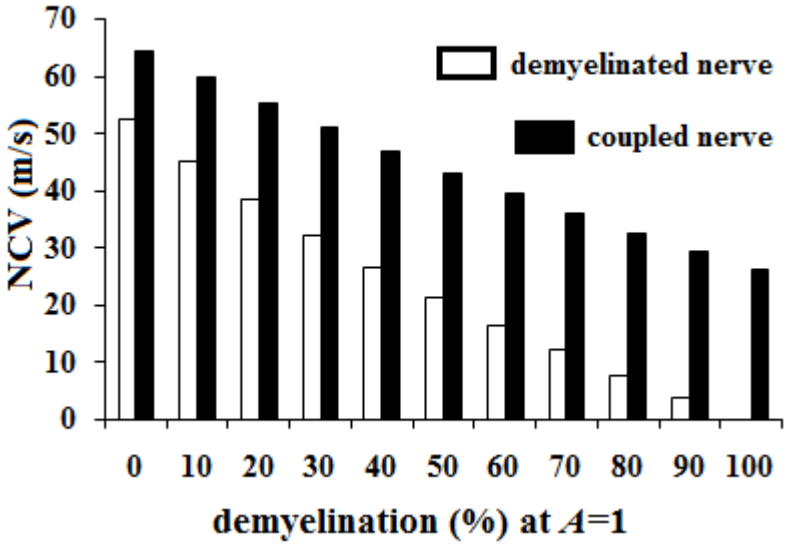

(b)

Figure 5.6: Theoretical estimation of NCV in demyelinated and coupled nerve in terms of alignment factor at (a) A=1/2 and (b) A=1.

5.4.2 Recovery in blocking of Na^+ and K^+ channels

In coupled nerve model, the action of Nk-PLA_2 of crude venom in sciatic nerve is suppressed by neurological properties of the normal nerves as obtained experimentally using Nk-PLA_2 (purified from crude venom). The CAP amplitude decreases with the increase of crude venom concentration due to having more number of channels blocking with increase of 3FTx content in crude venom. The coupling between Nk crude venom

treated nerve and normal nerve also shows increase in amplitude of both proximal and distal CAP (Fig-5.7(a) and (b)).

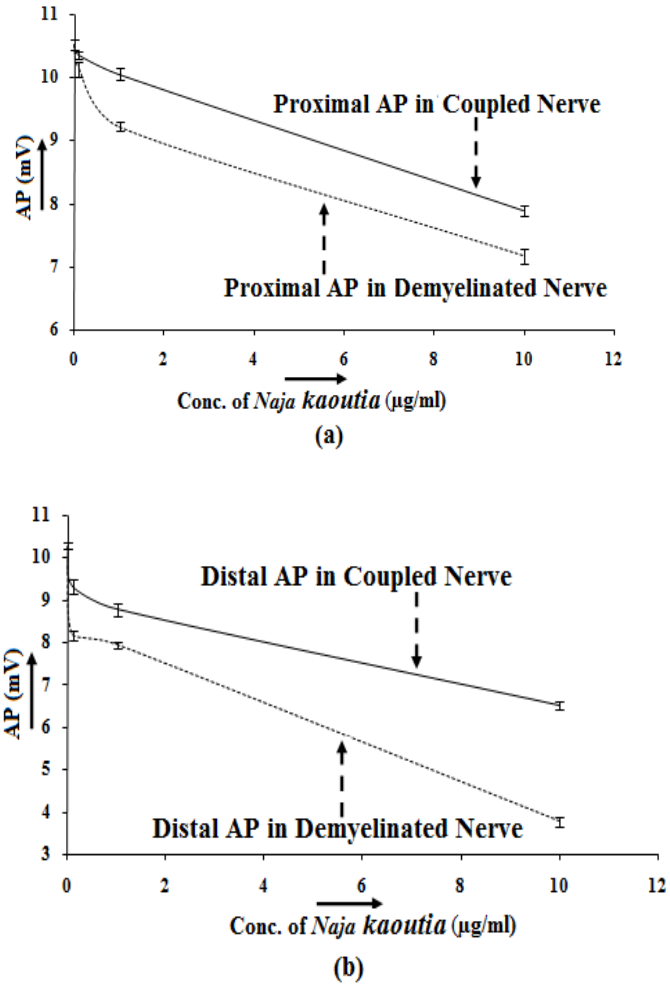

Figure 5.7: Comparison of AP in demyelinated and coupled nerve.

For demonstration of increase of CAP amplitudes only due to coupling, nerve conduction experiments are performed on 3FTx (purified from Nk crude venom) treated nerves. The reduction of both proximal and distal CAP amplitude is obtained due to blocking of 3FTx binding with nAch receptors (AchR). Neurotoxin 3FTx acting as an antagonist functions as a reverse for agonist Acetylcholine (Ach). The 3FTx binds tightly with the AchR at the postsynaptic membrane through covalent bond and forms 3FTx-AchR blocker (as shown in Fig-5.8(a)). It prevents the ionic channels from opening and thus blocks the transmission of ions through it. The percentage of proximal CAP amplitude reduction for 0.1µg/ml, 1.0µg/ml and 10µg/ml of 3FTx are ~15%, ~16%

and ~40% respectively whereas the percentage of reduced distal CAP amplitude are ~20%, ~27% and ~60%. As the concentration of 3FTx increases from 1µg/ml to 10µg/ml, the amplitude of both proximal and distal CAP decreases (Fig-5.7(a) and (b)) due to having more number of channel blocking.

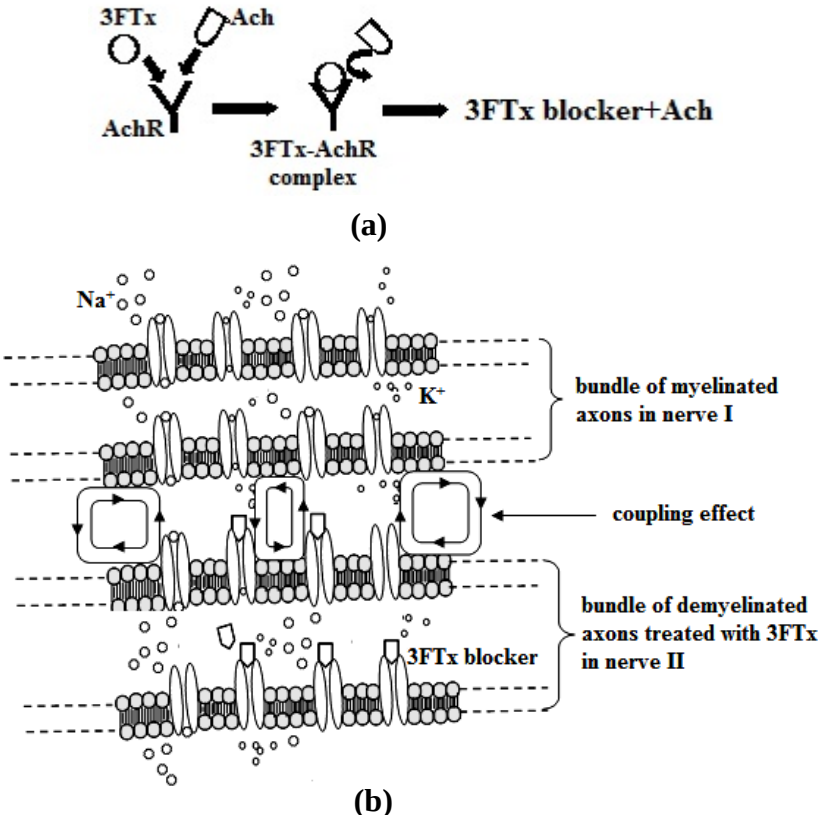

Figure 5.8: Blocking mechanism and coupling effect in coupled nerve.

The increases in both proximal and distal CAP amplitudes were made from nerve conduction experiments of coupled nerves. Correspondingly, the amplitudes of both proximal CAP increases by ~2%, ~9%, and ~11% whereas distal CAP amplitude are recovered by ~13%, ~27% and ~70% even if concentration of 3FTx increases from 0.1µg/ml to 10µg/ml due to suppression of electro dynamical activities of normal nerve over the demyelinated nerve as shown in Fig-5.8(b) and Table-5.4.

Table 5.4: Estimation of AP in nerves treated with 3FTx

No. of observations	Effect of 3Ftx	Estimation of AP (mV) for concentrations of 3FTx					
		0.1µg/ml		1µg/ml		10µg/ml	
		Distal AP	Proximal AP	Distal AP	Proximal AP	Distal AP	Proximal AP
I	Before coupling	8.3	10.0	8.0	9.3	3.8	7.2
II		8.2	10.1	7.9	9.2	3.9	7.3
III		8.2	10.2	8.0	9.2	3.9	7.3
IV		8.1	10.2	8.0	9.3	3.6	7.1
V		8.2	10.0	7.9	9.2	3.7	7.0
VI		8	10.3	7.8	9.1	3.7	7.1
A. P with SD		8.2±0.10	10.1±0.12	7.9±0.08	9.2±0.08	3.8±0.12	7.2±0.12
I	After coupling	9.1	10.3	8.5	10.1	6.6	8.0
II		9.3	10.4	8.9	10.0	6.4	7.9
III		9.5	10.4	8.9	10.1	6.6	7.8
IV		9.3	10.3	8.7	10.0	6.5	7.9
V		9.2	10.3	8.7	9.9	6.5	7.9
VI		9.5	10.4	8.9	10.2	6.4	7.8
A. P with SD		9.3±0.16	10.35±0.05	8.8±0.16	10.05±0.10	6.5±0.09	7.9±0.08

5.5 Discussions

Although all other experiments of ephaptic nerve coupling of demyelinated nerve with normal nerve are performed on sciatic nerves isolated from toad, the results open a recovery of neuro transmission via nerve coupling in malfunctioning nerve in human biopsy. The observations show experimental evidences for gradual recovery process to enhance slow NCV to its normal values and recovery of amplitude gain of neuro signal

due to coupling (as demonstrated in toad model of nerve coupling, Fig. 1(e)). The almost same results are obtained after performing nerve conduction experiments of coupled nerves (toad sciatic nerve treated with crude venom, Nk-PLA_2 and 3FTx neurotoxin separately with normal toad nerve) and NCV and CAP are estimated statistically with SD to minimize the percentage of error in the experimental results.

It is seen that the works provide experimental evidences of dysfunctions due to demyelination and its recovery in patients having different critical neuro diseases such as CIDP, GBS etc. Since the experiments are restricted to peripheral sciatic nerve, the coupling model extends to the recovery of neuro-transmission in motor nerve in Multiple Sclerosis (MS) and Epilepsy patient. So, the recovery model finds future scope in the treatment of neurological disorders with influence of normal neuro physiological properties of a normal adjacent nerve.

5.6 Conclusion

The increase in NCV obtained from electric circuit model of nerve fiber coupling shows similar results as obtained from experimental results of recovery of neuro-transmission. The neuro signals recorded from demyelinated nerves treated with 0.1µg/ml, 1µg/ml and 10µg/ml of Nk venom, the percentage of reduced NCV are obtained as ~19%, ~45 and ~52% for their corresponding venom concentrations. The percentage of NCV is recovered by ~34% for 0.1µg/ml, ~51% for 1µg/ml and ~54% for 10µg/ml of crude venom as the same nerve is coupled with a normal nerve. Similarly, for nerve treated with 0.1µg/ml, 1.0µg/ml and 10µg/ml of purified Nk-PLA_2, the percentage of NCV reduces by ~22%, ~48% and ~56%. When the nerve is coupled with a normal nerve, the percentage of increase in NCV is ~34%, ~53% and ~57% for 0.1µg/ml, 1.0µg/ml and 10µg/ml of Nk-PLA_2 in the coupled model. The percentage of proximal CAP amplitude reduction for 0.1µg/ml, 1.0µg/ml and 10µg/ml of 3FTx are ~15%, ~16% and ~40% respectively whereas the percentage of reduced distal CAP amplitude are ~20%, ~27% and ~60%. But in the coupled nerve, the amplitudes of both proximal CAP increases by ~2%, ~9%, and ~11% whereas distal CAP amplitude are recovered by ~13%, ~27% and ~70% respectively due to suppression of electro dynamical activities of normal nerve over the demyelinated nerve.

Bibliography

[1] Stephanova, D. L., Daskalova, M. S., and Alexandrov, A. S. Differences in membrane properties in simulated case of demyelinating neuropathies, intermodal focal demyelination with conduction block. *Journal of Biological Physics*, 32:129-144, 2006.

[2] Toothaker, T. B. and Brannagan, T. H. Chronic inflammatory demyelinating polyneuropathies: current treatment strategies. *Current Neurology and Neuroscience Reports*, 7 (1):63-70, 2007.

[3] Kuwabara, S. (2007). Guillain-Barre Syndrome. *Current Neurology and Neuroscience Reports*, 7(1):57-62, 2007.

[4] Berg, B. V. D., Walqaard, C., Drenthen, J., Fokee, C., Jacobs, B. C., and Doorn, P. A. V. Guillain-Barre syndrome: pathogenesis, diagnosis, treatment and prognosis. *Nature Reviews Neurology*, 10:469-482, 2014.

[5] Hoke, A. Mechanisms of disease: What factors limit the success of peripheral nerve regeneration in humans. *Nature Clinical Practice Neurology*, 2:448-454, 2006.

[6] Taveggia, C., Feltri, M. L., and Wrabetz, L. Signals to promote myelin formation and repair. *Nature Reviews Neurology*, 6:276-287, 2010.

[7] Susuki, K., Raphael, A. R., Oqawa, Y., Stankewich, M. C., Peles, E., Talbot, W. S., and Rasband, M. N. Schwann cell spectrins modulate peripheral nerve myelination. *Proceedings of the National Academy of Sciences*, 108(19):8009-8014, 2011.

[8] Pereira, J. A., Julein, F. L., and Suter, U. Molecular mechanisms regulating myelination in the peripheral nervous system. *Trends in Neuroscience*, 35(2):123-134, 2012.

[9] Chari, D. M. Remyelination in Multiple Sclerosis. *International Review of Neurobioliogy*, 79:589-620, 2007.

[10] Oqawa,Y., Sawamota, K., Miyata, T., and Okano, H. Transplantation of in vitro-expanded fetal neural progenitor cells results in neurogenesis and functional recovery after spinal cord contusion injury in adult rats. *Journal of Neuroscience Research*, 69:925-933, 2002.

[11] Wu. Y. P., Chen. W. S., Teng. C., and Zhang. N. Stem cells for the treatment of Neurodegenerative Diseases. *Molecules*, 15:6743-6758, 2010.

[12] Arvanitaki, A. Effects evoked in an axon by the activity of a contiguous one. *Journal of Neurophysiology*, 5:89-108, 1942.

[13] Bokil, H., Laaris, N., Blinder, K., Ennis, M., and Keller, A. Ephaptic Interactions in the Mammalian Olfactory System. *Journal of Neuroscience*, 21:1-5, 2011.

[14] Holt. G. R. and Koch. C. Electrical interactions via the extracellular potential near cell bodies. *Journal of Computational Neuroscience*, 6(2):169-184, 1999.

[15] Katz, B. and Schmitt, O. H. Electric interaction between two adjacent nerve fibers. Journal of Physiol, 97:471-488, 1940.

[16] Katz, B. and Schmitt, O. H. A note on interaction between nerve fibers, *Journal of Biophysics*, 100:369-371, 1942.

[17] Anastassiou, C. A., Perin, R., Markram, H., and Koch, C. Ephaptic coupling of cortical neurons. *Nature Neuroscience,* 14:217-223, 2011.

[18] Clark, J. W. and Plonsey, W. A. Mathematical Study of Nerve Fiber Interaction. *Biophysical Journal*, 10(10):937-957, 1970.

[19] Jiang, W., Chen, L., and Yang, F. X. Analysis and control of the bifurcation of Hodgkin Huxley model. *Chaos, Solitons & Fractals*, 31:247-256, 2007.

[20] Koles, Z. J. and Rasminsky, M. A computer simulation of conduction in demyelinated nerve fibers. Journal of Physiology, 227:351-364, 1972.

[21] Schnabel, V. and Johannes, J. S. Evaluation of the Cable Model for Electrical Stimulation of unmyelinated Nerve Fibers. *IEEE Transaction on Biomedical Engineering*, 48(9):1027-1033, 2001.